Influence of Fat on Liver T_1 Measurements Using Modified Look–Locker Inversion Recovery (MOLLI) Methods at 3T

Ferenc E. Mozes, MSc,[1]* Elizabeth M. Tunnicliffe, PhD,[1] Michael Pavlides, MD,[1,2] and Matthew D. Robson, PhD[1]

Purpose: To characterize the effect of fat on modified Look–Locker inversion recovery (MOLLI) T_1 maps of the liver. The balanced steady-state free precession (bSSFP) sequence causes water and fat signals to have opposite phase when repetition time (TR) = 2.3 msec at 3T. In voxels that contain both fat and water, the MOLLI T_1 measurement is influenced by the choice of TR.
Materials and Methods: MOLLI T_1 measurements of the liver were simulated using the Bloch equations while varying the hepatic lipid content (HLC). Phantom scans were performed on margarine phantoms, using both MOLLI and spin echo inversion recovery sequences. MOLLI T_1 at 3T and HLC were determined in patients ($n = 8$) before and after bariatric surgery.
Results: At 3T, with HLC in the 0–35% range, higher fat fraction values lead to longer MOLLI T_1 values when TR = 2.3 msec. Patients were found to have higher MOLLI T_1 at elevated HLC ($T_1 = 929 \pm 97$ msec) than at low HLC ($T_1 = 870 \pm 44$ msec).
Conclusion: At 3T, MOLLI T_1 values are affected by HLC, substantially changing MOLLI T_1 in a clinically relevant range of fat content.

J. MAGN. RESON. IMAGING 2016;44:105–111.

THE MODIFIED LOOK–LOCKER INVERSION RECOVERY (MOLLI)[1] T_1 mapping technique and variants of it have been gaining interest in cardiovascular magnetic resonance imaging (MRI)[2] and in liver imaging.[3] MOLLI is able to build a T_1 map within a breath-hold. It has also been demonstrated that MOLLI T_1 maps provide diagnostic information in the heart[4] and correlate with liver fibrosis and inflammation.[3]

Fat is known to have a short T_1, and in regions of visceral fat the MOLLI T_1 method measures this short T_1 with high reproducibility.[5] Similarly, the MOLLI T_1 method detects long T_1 regions of the blood pool with high reproducibility.[6] Patients suffering from liver-related diseases have been shown to have fat values in the 2% to 44% range[7–9]; thus, in livers with large amounts of fat, simplified reasoning would predict that the measured T_1 would be the weighted sum of the T_1 of the fat and the T_1 of the hepatic tissue. The measured T_1 of the liver would thus be expected to be reduced in fatty liver due to this partial volume effect. Phantom scans and previous work have demonstrated that T_1 decreases with increasing fat concentration when using conventional imaging methods, ie, spin echo inversion recovery (SE-IR).[10]

MOLLI T_1 values have been shown to be influenced by fat and off-resonance frequencies at 1.5T in the calf muscle[11] and the myocardium[12] and elevated MOLLI T_1 is often measured in patients with fatty livers[3] at 3T, where balanced steady-state free precession (bSSFP) repetition times (TRs) between 2.1 msec and 2.6 msec are commonly used.[3,13] It is the T_1 of the water component which appears to be of diagnostic significance when using T_1 mapping in the liver,[14] while the T_1 of the fat is constant[15] and not a predictor of disease. An important step towards the use of MOLLI T_1 to assess liver disease is the clarification and

View this article online at wileyonlinelibrary.com. DOI: 10.1002/jmri.25146

Received Sep 26, 2015, Accepted for publication Dec 21, 2015.

*Address reprint requests to: F.E.M., University of Oxford Centre for Clinical Magnetic Resonance Research (OCMR), University of Oxford, Level 0, John Radcliffe Hospital, Oxford, OX3 9DU, UK. E-mail: ferenc.mozes@cardiov.ox.ac.uk

From the [1]University of Oxford Centre for Clinical Magnetic Resonance Research (OCMR), University of Oxford, John Radcliffe Hospital, Oxford, UK; and [2]Translational Gastroenterology Unit, University of Oxford, John Radcliffe Hospital, Oxford, UK

quantification of the extent to which the presence of fat can mask or exaggerate changes in MOLLI T_1 due to disease.

The aim of this study was thus to investigate the effect of different fat concentrations and off-resonance frequencies on MOLLI T_1 maps at 3T with a bSSFP TR = 2.3 msec and to explain the mechanisms for this behavior.

Theory

MOLLI is an electrocardiogram (ECG)-gated inversion recovery T_1 mapping method. It uses several inversion pulses and acquires images synchronized to the cardiac cycle using a snapshot bSSFP[16] readout. Readouts are followed by pauses of a few heartbeats, allowing for full recovery of the longitudinal magnetization.[1]

The bSSFP readout results in images that are sensitive to the off-resonance frequency of the protons being imaged (Fig. 1).[17] The chemical shift difference between water and the main fat peak is 3.5 ppm,[18] which at 3T translates into a frequency difference of ~447 Hz. Therefore, if bSSFP images are acquired with a repetition time close to 1/447 seconds (~2.23 msec), the fat and water signals will have exactly opposite phase. When a different TR is chosen, the phase relationship between water and fat is a more complex function of off-resonance frequency.

The signal in a voxel containing both fat and water with no exchange of magnetization between them would be determined by the well-known partial volume effect. If the fat and water were in phase then the recovery would follow the sum of these two recovering exponentials; in practice, if this were fit to a single exponential then the measured T_1 would lie somewhere between the individual T_1s of the fat and the water. However, in the situation described in this work the water and fat are exactly out of phase, and so the signal recovery is the difference of two exponentials weighted by the relative contributions of fat and water. In practice, for relatively small fat concentrations this results in a measured value for T_1 that is longer than the T_1 value of either the fat or water component.[19] A conceptual schematic of this behavior is illustrated in Fig. 2.

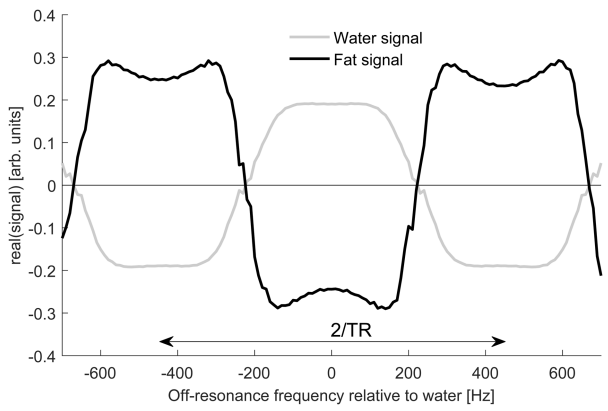

FIGURE 1: Variation of the steady-state signal over off-resonance frequencies relative to the water, as seen in Refs. 17 and 34. When a TR equal to the inverse of the chemical shift difference between water and fat is used, the steady-state signal of fat and water will have opposite phases.

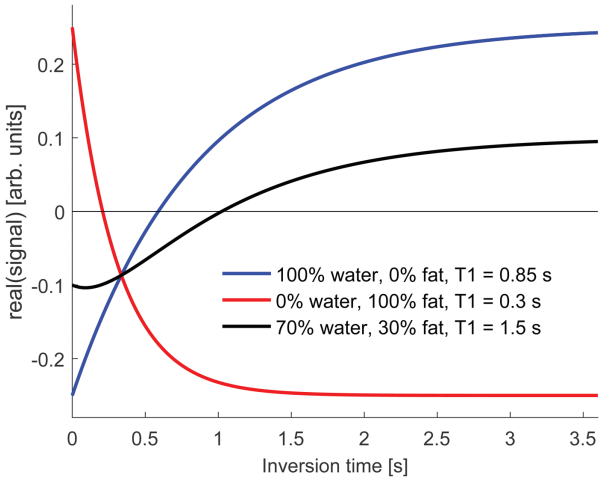

FIGURE 2: Schematic MOLLI recovery curves of water and fat components at identical main static field strength using TR = 2.3 msec. The 100% fat curve appears inverted because of its frequency shift. The different T_1 recovery times of fat and water and their opposing phases at TR = 2.3 msec lead to an apparent lengthening of the T_1 recovery in the combined signal.

Materials and Methods

Simulations

A Bloch equation[20] simulation was built in MatLab (MathWorks, Natick, MA) which emulated the exact pulse sequence of a MOLLI acquisition on our scanner. The simulated sequence included the waveforms of radiofrequency (RF) inversion, preparation, and imaging pulses. The measured signal intensity for each simulation was determined as the signal averaged over a set of phase encode lines centered on k = 25. Magnetization transfer effects were not included in the simulation, although they are known to bias T_1 with the MOLLI method.[21]

A single inversion followed by five image readouts was simulated, providing a good approximation to the MOLLI acquisition but eliminating the complexity that is due to the multitude of possible sampling schemes that have been described.[21] Since liver MOLLI T_1 values lie in the 700–1400 msec interval,[3] five samples over the recovery curve were used for determining the T_1.

The following simulation parameters were used: 3T field strength, 192 × 144 matrix, 84 phase encode lines, 24 phase encode lines before the central line, flip angle (FA) = 35°, TR/TE = 2.3/1.15 msec, TI = 100, 1000, 1900, 2800, 3700 msec, adiabatic hyperbolic secant 1 inversion pulse of 10.24 msec duration, time-bandwidth product of R = 5.48, peak B_1 = 750 Hz and β = 3.45.[21] The bSSFP readout used five linearly increasing startup angle (LISA) pulses[22,23] and one half-angle ramp down pulse.

T_1 and T_2 values for fat and liver components were: T_{1fat} = 382 msec, T_{2fat} = 68 msec,[24] $T_{1hepatic}$ = 812 msec,[25] $T_{2hepatic}$ = 34 msec.[24] Separate signals corresponding to each component of a multiple-peak lipid spectrum were weighted by their relative amplitude provided by Hamilton et al[26] and summed to obtain a single fat signal. Simulated fat and water signals were combined in

different proportions according to the principle of partial volumes and to reflect HLCs in the 0–100% range in steps of 1%, fat fractions, F, being defined using Eq. (1), where ρ_f and ρ_w denote the proton densities of fat and water.

$$F = \frac{\rho_f}{\rho_f + \rho_w} \times 100[\%] \quad (1)$$

Then, the signal points were fitted to an exponential describing longitudinal recovery, given by Eq. (2), where T_1^* is the apparent T_1 and A and B are additional fit parameters.

$$S(TI) = A - B\exp\left(-\frac{TI}{T_1^*}\right) \quad (2)$$

The MOLLI T_1 values were computed by using the imperfect,[27] but commonly used, Look–Locker correction method described by Eq. (3).[1]

$$T1 = T_1^*\left(\frac{B}{A} - 1\right) \quad (3)$$

In order to show the changes in MOLLI T_1 caused by repetition times other than 2.3 msec, the variation of MOLLI T_1 with off-resonance frequency was simulated for two repetition times found in the literature: TR = 2.14 msec[3] and TR = 2.6 msec.[13] All simulation parameters were the same as described above for the liver simulation, with the simplification that only three lipid concentrations were simulated: 0%, 10%, and 20%. The chosen off-resonance frequency range was –100 Hz to 100 Hz in steps of 2 Hz, which covers the typical frequency range encountered in the in vivo MOLLI data discussed below.

To further explore the effects of fat on MOLLI T_1 values, the TR was varied in a simulation comprising a water and a multiple-peak fat component with 30% fat fraction. The spectral model of the fat was based on the ^{1}H spectrum of the margarine phantom described below. The same imaging protocol was simulated as described in the previous section, with the following differences: TI = 200, 1200, 2200, 3200, 4200 msec, RR = 1000 msec, and 31 bSSFP TR values in the range 1.93 to 5.75 msec. T_1 and T_2 values for fat and water components corresponded to those of a margarine phantom and were T_{1fat} = 325 msec, T_{2fat} = 120 msec, T_{1water} = 2448 msec, and T_{2water} = 207 msec. The measurements leading to these values are described in the next section.

Phantom Scans

Phantom experiments were carried out using a margarine phantom (Flora Light, Unilever) with 30% fat content. First, the margarine phantom was scanned using a 5-point MOLLI sequence. Imaging parameters followed a standardized MOLLI acquisition protocol (Siemens WIP 561a, Erlangen, Germany): 192 × 144 matrix, FA = 35°, TR/TE = 2.3/0.99 msec, TI = 100, 1100, 2100, 3100, 4100 msec, simulated ECG with RR = 1000 msec. Then the same margarine phantom was scanned using the SE-IR sequence. Imaging parameters followed a standardized acquisition protocol: 128 × 128 matrix, TR = 10000 msec, TI = 50, 150, 250, 400, 600, 900, 1300, 2000, 3000, 4500, 6500 msec, TE = 7.4 msec. In both cases images were acquired using a Siemens 3T Verio scanner using a 32-channel head RF coil.

Following the margarine scans, a sample of the margarine was heated and then spun with a centrifuge (Rotanta 460R, Hettich) at 4000 rpm for 5 minutes. After spinning the sample, separate layers of fat and water were obtained that were scanned using the MOLLI acquisition and the SE-IR acquisition using the same scanner and same protocols as described above.

A subsequent experiment was carried out in order to determine MOLLI T_1 of the whole margarine and the water component only over a range of repetition times. The previously described 5-point MOLLI acquisition protocol was used with the following changes: TI = 200, 1200, 2200, 3200, 4200 msec, RR = 1000 msec, and 31 bSSFP TR values ranging from 1.93 to 5.75 msec.

MOLLI T_1 values were determined by fitting the signal intensity of a circular region of interest on the bSSFP images following the inversion pulse to Eq. (2), then applying Eq. (3) to obtain T_1. T_1 values for images acquired using the SE-IR sequence were computed by fitting Eq. (4) to mean signal values sampled from the same region of interest in each image.

$$S(TI) = C\left(1 - 2\exp\left(-\frac{TI}{T_1}\right) + \exp\left(-\frac{TR}{T_1}\right)\right) \quad (4)$$

Patient Studies

In order to compare the results of the simulations to results obtained in vivo, data from eight patients (seven female, mean age: 49 ± 10.5 years) were processed retrospectively. Patients were scanned before weight reduction surgery and 6 months postoperatively. Relevant parameters of the patients before surgery included mean body mass index (BMI): 45.8 ± 5.5 kg/m^2, mean waist circumference: 120.25 ± 10.35 cm, and mean hip circumference: 134.5 ± 11.2 cm. Four of the patients suffered from diabetes. Postoperative parameters were: mean BMI: 36.4 ± 4.8 kg/m^2, mean waist circumference: 107.7 ± 10.6 cm, and mean hip circumference: 120.6 ± 8.6 cm.

The study protocol conformed to the ethical guidelines of the 1975 Declaration of Helsinki, and was approved by the institutional research departments and the National Research Ethics Service (13/SC/0243). All patients gave written informed consent.

At each timepoint, patients had liver MOLLI T_1 maps (5-point MOLLI was employed). T_2* maps were collected for hepatic iron quantification and ^{1}H MRS for the quantification of liver fat using the stimulated echo acquisition mode (STEAM) sequence. Imaging parameters for the MOLLI scan were: 192 × 134–160 matrix (depending on patient), field of view (FOV) 280–348 × 350–500 mm (depending on patient), slice thickness of 8 mm, GRAPPA acceleration factor 2, pixel bandwidth 898 Hz/px, TR/TE = 2.14/1.07 msec, FA = 35°, TI = 110, 110+RR, 110+2RR, 110+3RR, 110+4RR msec. MOLLI T_1 maps were acquired in transverse scan planes.

T_2* maps were determined using a multiecho acquisition with RF spoiling. Imaging parameters for this acquisition were as follows: same FOV as for the 5-point MOLLI sequence, 192 × 128–160 matrix (depending on patient), slice thickness of 3 mm, GRAPPA acceleration factor 2, TR/TE = 26.5/2.46, 7.38, 12.30,

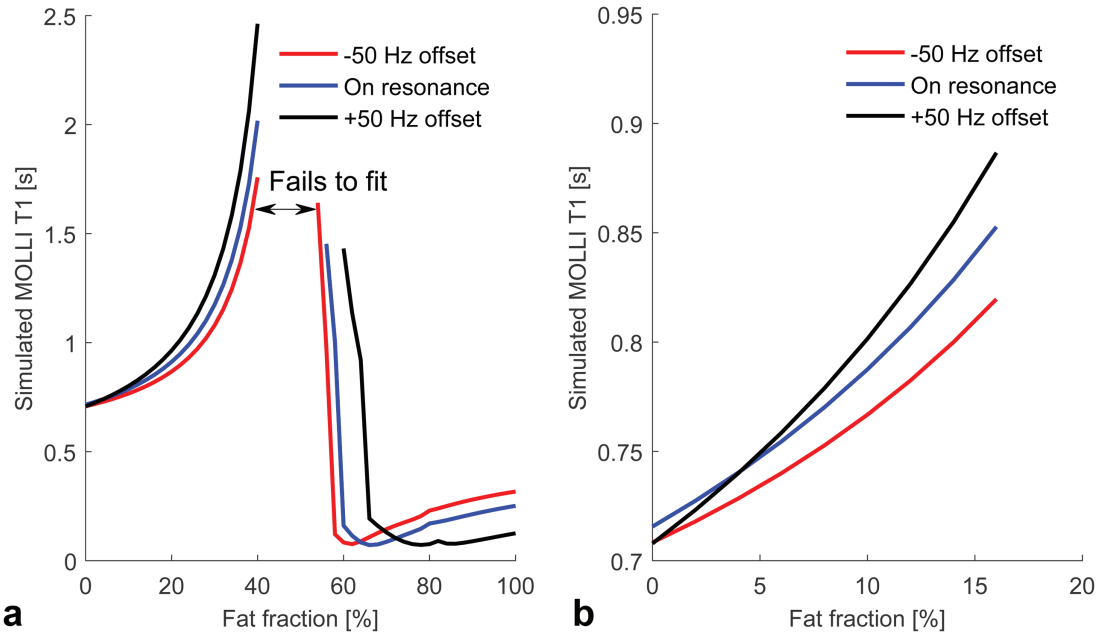

FIGURE 3: Variation of simulated MOLLI T_1 values of the liver with fat fraction emphasizing behavior at off-resonance: (a) global behavior of MOLLI T_1 values over the full range of fat fractions; (b) MOLLI T_1 behavior corresponding to the 0–16% range of fat fractions.

17.22, 22.14 msec, FA = 20°. Fat saturation and double-inversion black blood preparation were used.

The STEAM spectroscopy experiment used[28]: TE = 10 msec, TM = 7 msec, TR = 2 seconds for water-suppressed spectra and TR = 4 seconds for water-unsuppressed spectra and voxel volume was 8 cm^3. The voxel of interest was placed in the lateral part of the right lobe of the liver, avoiding vessels, bile ducts, and the edge of the liver. Spectra were processed using AMARES in jMRUI[29] with a specialized MatLab script[28] and the fat fraction was determined as the ratio of the fat signal and the sum of the fat and water signals as in Eq. (1).

Results

Simulation

Figure 3 presents the relationship between the simulated MOLLI T_1 and HLC. At low HLC (0–16% range) the measured MOLLI T_1 increases with increasing fat, and can be approximated by:

$$MOLLI\ \ T_1 = 715 + 5.47F + 0.27F^2 \qquad (5)$$

where MOLLI T_1 is expressed in milliseconds and F is the percent HLC. This trend ends at approximately $F = 40\%$, where fitting becomes impossible owing to the water signal and fat signal canceling each other out. For $F > 50\%$ the MOLLI T_1 values change rapidly, eventually reaching the T_1 of the fat at 100% fat fraction. The increase of MOLLI T_1 is explained by the simultaneous increase of both the B/A ratio and the apparent T_1 (T_1*) in Eq. (3).

Figure 3 also presents the behavior of MOLLI T_1 variation in the case of off-resonance. Although the bSSFP

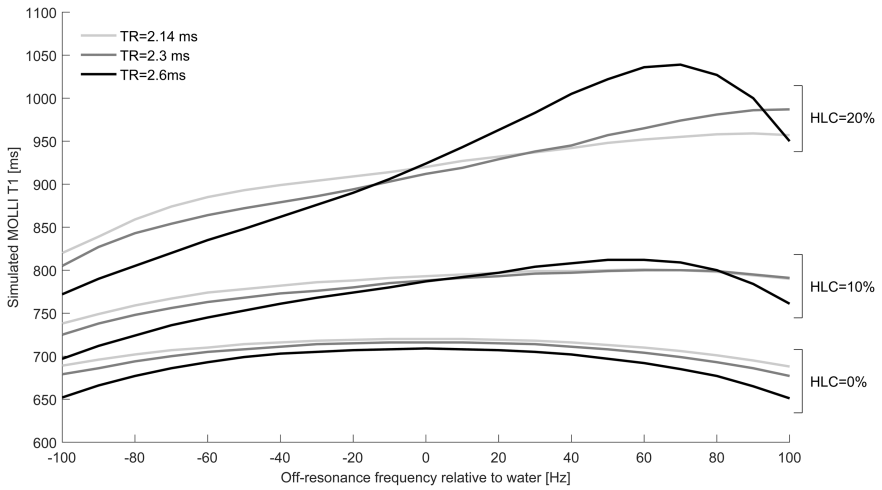

FIGURE 4: Variation of simulated MOLLI T_1 with off-resonance frequency and using repetition times described in the literature.[3,13]

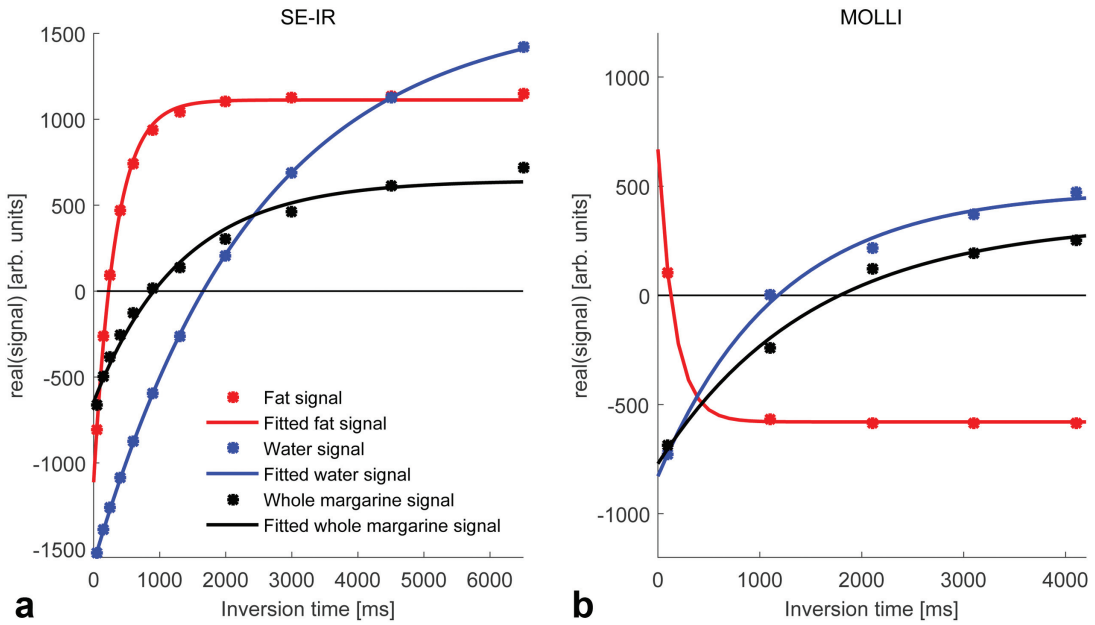

FIGURE 5: Fitted T_1 recovery curves of whole margarine, fat component, and water component in the 30% fat margarine phantom: (a) shows the results of the spin echo inversion recovery experiment; (b) shows the results of the MOLLI experiment.

readout leads to a symmetric MOLLI T_1 variation around the central water frequency for 0% HLC, using a multiple-peak spectral model of the lipid leads to asymmetric off-resonance frequency dependence.

In simulations the dependence of MOLLI T_1 on off-resonance frequency when using repetition times from the literature[3,13] is shown in Fig. 4. Simulated MOLLI T_1 values were found to be higher at lower repetition times for most fat fractions and off-resonance frequencies. In addition, MOLLI T_1–off-resonance frequency dependence is both larger and increasingly asymmetric with respect to frequency in the presence of higher fat.

Phantom Scans

T_1 values determined from MOLLI and SE-IR experiments in the margarine phantom are presented in Table 1.

Figure 5 shows the signal intensities taken from regions of interest on SE-IR images and the curves fitted to these points, along with the signal intensities sampled from MOLLI acquisitions and corresponding fitted curves.

TABLE 1. T_1 Values Measured by the MOLLI Method and Computed From SE-IR Images

Phantom type	30% margarine	
	MOLLI T_1 [msec]	SE-IR T_1 [msec]
Whole margarine	3874 ± 177	1313 ± 14
Fat component	291 ± 23	325 ± 20
Water component	2266 ± 21	2448 ± 7

The results of the simulation and phantom experiment exploring the dependence of MOLLI T_1 on repetition times is shown in Fig. 6. Both simulated and measured MOLLI T_1 values of the margarine phantom with 30% fat were higher than those of water over the 1.8 to 3.5 msec range and lower over the 3.5 to 5.75 msec range due to the relative position of the bSSFP profiles of the fat and water. However, the simulated and measured data did not agree perfectly. A possible explanation for the mismatch could be the missing information on the different T_1 and T_2 values of the individual fat peaks in the margarine phantom. A similar difference between simulation and phantom experiments can be seen in Thiesson et al's work.[11]

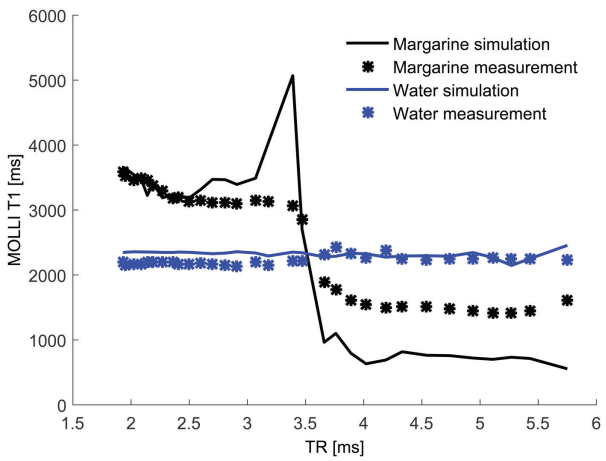

FIGURE 6: Variation of MOLLI T_1 with the change of TR. Fat and water are out of phase at TR = 2.3 msec and in phase at TR = 4.6 msec.

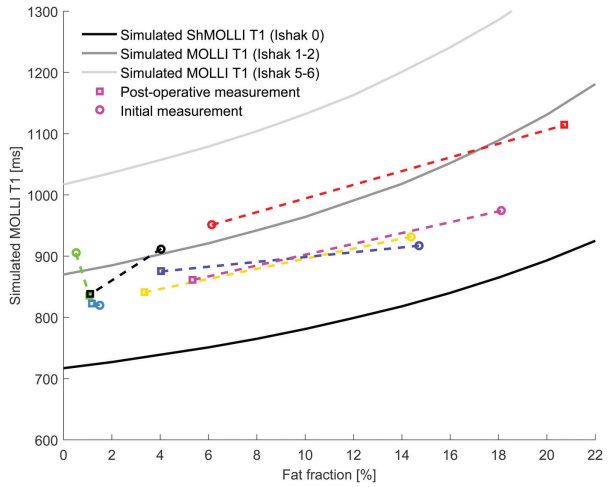

FIGURE 7: Continuous lines represent the variation of simulated MOLLI T_1 with HLC, for three levels of liver fibrosis as defined by the Ishak score. These curves were obtained by running the simulation for T_1 values corresponding to different disease states as described by Banerjee et al[3] (see their fig. 2). Dashed line segments connect patient data points, showing the change in measured MOLLI T_1 for each individual.

Patient Studies

One patient was excluded from the comparison because the T_1 fit to the MOLLI data failed at the first visit. The measured HLC for this patient was 39.7%, which is in the regime where the Bloch simulated data could also not be fitted to an inversion recovery model.

Six patients had normal T_2* values larger than 19 msec and one had T_2* = 15 msec, indicating elevated iron but all within the normal range for T_2* at 3T.[30]

Pre- and postoperative MOLLI T_1 measurements for seven patients are shown in Fig. 7, plotted as a function of their spectroscopically measured HLC. Simulated relationships between T_1 and HLC are also included for three different levels of liver fibrosis, characterized by the Ishak score.[31] MOLLI T_1 values at 0% HLC for the three curves were taken from Banerjee et al, as shown in their fig. 2 of Ref. 3. The changes in MOLLI T_1 that occur in these patients are consistent with the hypothesis that the water in the livers of these patients is elevated but stable between exams and that the fat concentration has changed. These patients are expected to have some level of inflammation or fibrosis, which has previously been shown to elevate MOLLI T_1.[3]

Discussion

In a physiological range of HLC from 0% to 45%[7–9] we have shown that the MOLLI T_1 at 3T increases with fat concentration in simulation and phantoms when using TR = 2.3 msec. This also applies when TR lies in the range 2.1 to 2.6 msec. The MOLLI T_1 elevation is seen in vivo with the caveat that there may be other changes in the livers of the patients over 6 months after bariatric surgery that would be expected to modify the T_1.[3]

Due to a chemical shift difference of 447 Hz between fat and water at 3T, the two tissue components are exactly out of phase with their passbands overlapping when using TR = 2.3 msec. Thus, combined signals from tissue containing fat and water are less dependent on off-resonance frequency than reported previously using TR = 2.7 msec at 1.5T.[11] Increasing or decreasing the TR from 2.3 msec at 3T reduces the overlap of the two bSSFP passbands, increasing the off-resonance frequency dependence.

These simulations suggest that careful shimming, in addition to the use of a TR of 2.3 msec or less, is useful to maximize the consistency of MOLLI T_1 measurements within a single subject and between subjects.

In contrast to 3T, where the optimal TR for reducing the frequency dependence of MOLLI T_1 measurements is close to the minimum TR available with existing hardware, at 1.5T longer TR values would have to be used to produce a similar overlapping of the two bSSFP passbands due to the smaller chemical shift difference between fat and water.[32]

Patient MOLLI T_1 evolution in a 6-month interval after bariatric surgery follows our model describing the influence of fat on MOLLI T_1 values. We expect that, while the amount of fat changes in these patients, other parameters known to affect the T_1 (such as fibrosis and inflammation) remain fairly constant. In general terms, the change in measured MOLLI T_1 is consistent with the behavior that is predicted by the simulation for changes in liver fat in five of the seven patients; in one patient the change in liver fat is very small and the MOLLI T_1 change is small, and in one patient the liver fat change is small, but the MOLLI T_1 change is ~100 msec, not following the model. We believe that this supports the applicability of the model in vivo.

A limitation of this study is the small size of the patient cohort. A change in MOLLI T_1 in two of the patients was not explained by change in fat fractions, suggesting the existence of other mechanisms responsible for having an influence on hepatic MOLLI T_1 values.

The MOLLI T_1 mapping method is used extensively in cardiac imaging and so it is important to briefly consider the effect of myocardial fat on MOLLI T_1 maps at 3T. Since global lipid fractions in the myocardium are in the 0.2–2% interval,[28,33] they have a much smaller effect on measured MOLLI T_1 values. An exception is in focal lipid accumulations, which can be as high as 35% in the case of lipomatous metaplasia,[12] leading to replacement of scar tissue with lipid accumulations after myocardial infarction. Effects of these focal lipid concentrations are described by Kellman et al.[12]

In conclusion, this study has shown that the presence of fat influences MOLLI T_1 measurements in the liver. This effect is in addition to the previously known effects of T_2, magnetization transfer, off-resonance frequency, and iron concentration. Simulation has shown that fat fractions up to 40% will have an additive effect on the measured MOLLI T_1 value at 3T when using a bSSFP readout with TR = 2.3

msec. This behavior has been confirmed in the livers of patients undergoing weight-reduction surgery.

The influence of fat should be considered in the assessment of hepatic diseases using MOLLI T_1 measurements, as fat fraction values measured in the liver can be large enough to cause severe MOLLI T_1 alterations.

Acknowledgment

Contract grant sponsor: UK Medical Research Council Doctoral Training Award; Contract grant sponsor: Scatcherd European Scholarship; Contract grant sponsor: The RDM Scholars Programme; Contract grant sponsor: The National Institute for Health Research (NIHR) Oxford Biomedical Research Centre Programme.
The views expressed are those of the authors and not necessarily those of the NHS, the NIHR or the Department of Health.

References

1. Messroghli DR, Radjenovic A, Kozerke S, Higgins DM, Sivananthan MU, Ridgway JP. Modified Look-Locker inversion recovery (MOLLI) for high-resolution T1 mapping of the heart. Magn Reson Med 2004;52:141–146.
2. Moon JC, Messroghli DR, Kellman P, et al. Myocardial T1 mapping and extracellular volume quantification: a Society for Cardiovascular Magnetic Resonance (SCMR) and CMR Working Group of the European Society of Cardiology consensus statement. J Cardiovasc Magn Reson 2013;15:92.
3. Banerjee R, Pavlides M, Tunnicliffe EM, et al. Multiparametric magnetic resonance for the non-invasive diagnosis of liver disease. J Hepatol 2014;60:69–77.
4. Ferreira VM, Piechnik SK, Robson MD, Neubauer S, Karamitsos TD. Myocardial tissue characterization by magnetic resonance imaging: novel applications of T1 and T2 mapping. J Thorac Imaging 2014;29:147–154.
5. Ferreira VM, Holloway CJ, Piechnik SK, Karamitsos TD, Neubauer S. Is it really fat? Ask a T1-map. Eur Heart J Cardiovasc Imaging 2013;14:1060.
6. Vassiliou V, Heng EL, Sharma P, et al. Reproducibility of T1 mapping 11-heart beat MOLLI Sequence. J Cardiovasc Magn Reson 2015;17(Suppl 1): W26.
7. Bannas P, Kramer H, Hernando D, et al. Quantitative magnetic resonance imaging of hepatic steatosis: validation in ex vivo human livers. Hepatology 2015;62:1444–1455.
8. Tang A, Tan J, Sun M, et al. Nonalcoholic fatty liver disease: MR imaging of liver proton density fat fraction to assess hepatic steatosis. Radiology 2013;267:422–431.
9. Idilman IS, Aniktar H, Idilman R, et al. Hepatic steatosis: quantification by proton density fat fraction with MR imaging versus liver biopsy. Radiology 2013;267:767–775.
10. Rakow-Penner R, Daniel B, Yu H, Sawyer-Glover A, Glover GH. Relaxation times of breast tissue at 1.5T and 3T measured using IDEAL. J Magn Reson Imaging 2006;23:87–91.
11. Thiesson S, Thompson R, Chow K. Characterization of T1 bias from lipids in MOLLI and SASHA pulse sequences. J Cardiovasc Magn Reson 2015;17(Suppl 1):W10.
12. Kellman P, Bandettini WP, Mancini C, Hammer-Hansen S, Hansen MS, Arai AE. Characterization of myocardial T1-mapping bias caused by intramyocardial fat in inversion recovery and saturation recovery techniques. J Cardiovasc Magn Reson 2015;17:33.
13. de Meester de Ravenstein C, Bouzin C, Lazam S, et al. Histological validation of measurement of diffuse interstitial myocardial fibrosis by myocardial extravascular volume fraction from modified Look-Locker imaging (MOLLI) T1 mapping at 3 T. J Cardiovasc Magn Reson 2015;17:48.
14. Leporq B, Ratiney H, Pilleul F, Beuf O. Liver fat volume fraction quantification with fat and water T1 and T2* estimation and accounting for NMR multiple components in patients with chronic liver disease at 1.5 and 3.0 T. Eur Radiol 2013;23:2175–2186.
15. Hamilton G, Middleton MS, Hooker JC, et al. In vivo breath-hold (1) H MRS simultaneous estimation of liver proton density fat fraction, and T1 and T2 of water and fat, with a multi-TR, multi-TE sequence. J Magn Reson Imaging 2015;42:1538–1543.
16. Bieri O, Scheffler K. Fundamentals of balanced steady state free precession MRI. J Magn Reson Imaging 2013;38:2–11.
17. Scheffler K, Lehnhardt S. Principles and applications of balanced SSFP techniques. Eur Radiol 2003;13:2409–2418.
18. Yu H, McKenzie CA, Shimakawa A, et al. Multiecho reconstruction for simultaneous water-fat decomposition and T2* estimation. J Magn Reson Imaging 2007;26:1153–1161.
19. Kellman P, Wilson JR, Xue H, Ugander M, Arai AE. Extracellular volume fraction mapping in the myocardium. Part 1: Evaluation of an automated method. J Cardiovasc Magn Reson 2012;14:63.
20. Brown RW, Cheng Y-CN, Haacke EM, Thompson MR, Venkatesan R (eds.). Magnetization, relaxation, and the Bloch equation. In: Magnetic resonance imaging: physical principles and sequence design, 2nd ed. Hoboken, NJ: John Wiley & Sons; 2014. p 53–66.
21. Robson MD, Piechnik SK, Tunnicliffe EM, Neubauer S. T1 measurements in the human myocardium: The effects of magnetization transfer on the SASHA and MOLLI sequences. Magn Reson Med 2013;70:664–670.
22. Nishimura DG, Vasanawala SS. Analysis and Reduction of the Transient Response in SSFP Imaging. In: Proc 8th Annual Meeting ISMRM, Denver; 2000:301.
23. Deshpande VS, Shea SM, Laub G, Simonetti OP, Finn JP, Li D. 3D magnetization-prepared true-FISP: a new technique for imaging coronary arteries. Magn Reson Med 2001;46:494–502.
24. de Bazelaire CMJ, Duhamel GD, Rofsky NM, Alsop DC. MR imaging relaxation times of abdominal and pelvic tissues measured in vivo at 3.0 T: preliminary results. Radiology 2004;230:652–659.
25. Stanisz GJ, Odrobina EE, Pun J, et al. T1, T2 relaxation and magnetization transfer in tissue at 3T. Magn Reson Med 2005;54:507–512.
26. Hamilton G, Yokoo T, Bydder M, et al. In vivo characterization of the liver fat ^{1}H MR spectrum. NMR Biomed 2011;24:784–790.
27. Deichmann R, Haase A. Quantification of T1 values by SNAPSHOT-FLASH NMR imaging. J Magn Reson 1992;96:608–612.
28. Rial B, Robson MD, Neubauer S, Schneider JE. Rapid quantification of myocardial lipid content in humans using single breath-hold 1H MRS at 3 Tesla. Magn Reson Med 2011;66:619–624.
29. Naressi A, Couturier C, Devos JM, et al. Java-based graphical user interface for the MRUI quantitation package. Magma Magn Reson Mater Phys Biol Med 2001;12:141–152.
30. Storey P, Thompson AA, Carqueville CL, Wood JC, de Freitas RA, Rigsby CK. R2* imaging of transfusional iron burden at 3T and comparison with 1.5T. J Magn Reson Imaging 2007;25:540–547.
31. Ishak K, Baptista A, Bianchi L, et al. Histological grading and staging of chronic hepatitis. J Hepatol 1995;22:696–699.
32. Hargreaves BA, Vasanawala SS, Nayak KS, Hu BS, Nishimura DG. Fat-suppressed steady-state free precession imaging using phase detection. Magn Reson Med 2003;50:210–213.
33. Liu C-Y, Bluemke DA, Gerstenblith G, et al. Myocardial steatosis and its association with obesity and regional ventricular dysfunction: evaluated by magnetic resonance tagging and 1H spectroscopy in healthy African Americans. Int J Cardiol 2014;172:381–387.
34. Bernstein MA. Basic pulse sequences. In: Bernstein MA, King KF, Zhou XJ, editors. Handbook of MRI pulse sequences, 1st ed. Amsterdam: Elsevier; 2004. p 594.